Tetrahedron: *Asymmetry* 19 (2008) 2390–2395

Contents lists available at ScienceDirect

Tetrahedron: *Asymmetry*

journal homepage: www.elsevier.com/locate/tetasy

(5′*R*)-5′,8-Cyclo-2′-deoxyadenosine: NMR and DFT study of its influence on T_{PO}cdA structure

Bolesław T. Karwowski *

Department of Biopharmacy, Medical University of Lodz, Muszyńskiego Street 1, 90-151, Łódź, Poland

ARTICLE INFO

Article history:
Received 1 September 2008
Accepted 23 October 2008
Available online 19 November 2008

ABSTRACT

Oxidatively generated damage to DNA frequently appears in the human genome as an effect of aerobic metabolism or as the result of exposure to *exo*genous oxidizing agents, such as ionizing radiation and solar light, a product of radiation. 5′,8-Purine cyclonucleosides constitute an important class of oxidatively generated tandem lesions. The present study deals with the synthesis of the (5′*R*)-diastereomer of 5′,8-cyclo-2′-deoxyadenosine (cdA) containing T_{PO}cdA, in an attempt to delineate the conformational changes induced in the DNA fragments by the presence of this lesion. For this purpose, extensive 1D and 2D NMR measurements were performed and completed by theoretical calculations. It was found that the covalent bond between C(5′) and C(8) in the (5′*R*)-5′,8-cyclo-2′-deoxyadenosine induces an unusual West ($_0T^1$) conformation of the furanose ring. It is similar to the opposite (5′*S*)-diastereoisomer; however, the three-dimensional structure of the dinucleoside investigated has shown an analogy to natural d(T_{PO}A). Thus, it can be postulated that the rigid structure of (5′*R*)-5′,8-cyclo-2′-deoxyadenosine would perturb the global geometry of oligonucleotides at the site of the modification less strongly than (5′*S*) and therefore be less toxic for cells. In this article, the influence of the (5′*R*)-diastereomer of 5′,8-cyclo-2′-deoxyadenosine on the dinucleotide structure will be presented for the first time.

1. Introduction

Nucleotides and nucleosides in the natural environment are constantly exposed to different kinds of radicals.[1] Among them the major portions are hydroxyl radicals formed in cells as a result of water γ-radiolysis, or during anaerobic cellular processes.[2] The reactions of a radical with oligonucleotides and nucleosides may lead to nucleic base modifications or other DNA lesions, including strand breaks. The majority of them can be removed during the BER repair process.[3] However, modifications which involved simultaneous damage of the sugar residue and of the base (tandem lesions)—for example, 5′,8-cyclo-2′-deoxyadenosine (cdA)—are not eliminated by the BER (base excision repair) system, but by the complex NER (nucleotide excision repair) system.[4] Experimental data show that (*R*)- and (*S*)-diastereomers of cdA are formed in a 2:1 ratio for free nucleoside and 1:1 in the case of oligonucleotides.[5] Moreover, depending on the C5′ atom configuration in cdA as (*R*) or (*S*) (Fig. 1), they are characterized with a different biological impact.[6] For example, (5′*S*)-5′,8-cyclo-2′-deoxyadenosine completely blocks the progression of polymerases involved in

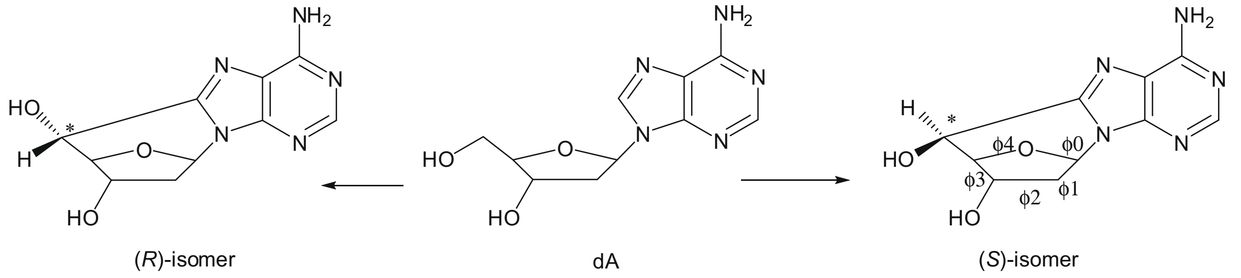

Figure 1. The (5′*R*)- and (5′*S*)-diastereomers of 5′,8-cyclo-2′-deoxyadenosine with indication of torsion angles in the furanose ring by symbols ϕ_0, ϕ_1, ϕ_2, ϕ_3, ϕ_4.

---

* Tel.: +48 42 677 91 21; fax: +48 42 677 91 20.
E-mail address: Bolek.Karwowski@wp.pl

0957-4166/$ - see front matter © 2008 Elsevier Ltd. All rights reserved.
doi:10.1016/j.tetasy.2008.10.025

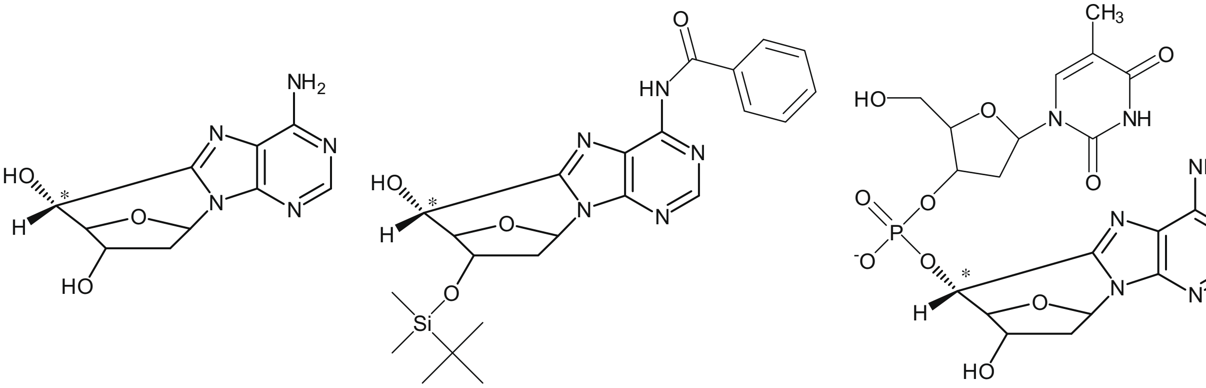

1 **2** **3**

Figure 2. Structure of (5′*R*)cdA **1**, (5′*R*)cdA$^{\mathrm{NBz}}_{\mathrm{TBDMSi}}$ **2**, T$_{\mathrm{PO}}$(5′*R*)cdA **3**.

oligonucleotide chain extension, whereas the (5′*R*)-diastereomer has a less pronounced effect.[7] Moreover, the (5′*R*)-form was found to be more efficiently removed from cdA containing oligonucleotides than the (5′*S*)-diastereomer via an NER mechanism.

The present study is aimed at delineating the conformational features of the (5′*R*)-diastereomer of either free cdA **1**, the O-3′ and N-6 cdA-substituted derivative *N*^{6}-benzoyl-3′-*O*-(*tert*-butyldimethylsilyl)-5′,8-cyclo-5′-oxo-2′-eoxyadenosine (cdA$^{\mathrm{NBz}}_{\mathrm{TBDMSi}}$) **2**, or when inserted into a dinucleotide, namely T$_{\mathrm{PO}}$cdA **3** (Fig. 2). This was achieved by both extensive NMR studies in aqueous solutions and theoretical DFT (density functional theory) calculations.

2. Results and discussion

2.1. Synthesis of cdA$^{\mathrm{NBz}}_{\mathrm{TBDMSi}}$, cdA and cdA containing dinucleotide

(5′*R*)-5′,8-Cyclo-2′-deoxyadenosine **1**, cdA$^{\mathrm{NBz}}_{\mathrm{TBDMSi}}$ **2** and their derivatives for short oligonucleotides synthesis were obtained by the method described by Cadet.[8] The T$_{\mathrm{PO}}$cdA **3** was synthesized via solid-phase synthesis on the 1 μmol scale using a classical phosphoamidite strategy[9] with a slight modification as reported by Brooks.[10] The synthetic products were purified by a one-step purification method using RP-HPLC DMT$^{\mathrm{OFF\ level}}$.

2.2. Molecular structure of cdA, cdA$^{\mathrm{NBz}}_{\mathrm{TBDMSi}}$, T$_{\mathrm{PO}}$cdA from DFT studies

It should be noted that X-ray data are only available for both the (5′*R*)- and (5′*S*)-diastereoisomers of the ribofuranose-derivatives of cA (5′,8-cyclo adenosine).[11] Therefore, quantum mechanics was chosen for the DFT calculations[12] with the goal of cross-checking the experimental data obtained from NMR. It has been found that the conformation of the fixed sugar ring is independent of the presence of substituents. The torsion angles and the distances in cdA are similar to those formed in cA. Moreover, I have not observed any changes in the (5′*R*)-5′,8-cyclo-2′-deoxyadenosine structure, independent of whether it has been modelled as the cdA monomer, cdA$^{\mathrm{NBz}}_{\mathrm{TBDMSi}}$, or as conjugates such as T$_{\mathrm{PO}}$cdA. Surprisingly, the crystallographic structural data[11] of cA were consistent with data inferred from the quantum chemical calculations for all structures studied that exhibit the $_0T^1$ conformation for the sugar moiety. The homology of the conformation of the furanose ring forced the position of adenine in relation to the sugar unit. Therefore, the values of the glycosidic dihedral angle (O4′–C1′–N9–C4) between both 5′*R* and 5′*S* diasrereoizomers differ only by 4.1°. Additionally, this difference has been determined by the position of the 5′OH group and moreover, the value of the newly created C3′–C4′–C5′–C8 dihedral angel is almost the same for 5′*S* and 5′*R* forms. Another point to be noted from the DFT calculations is that the 5′-furanose ring from thymidine adopts the ($^2T_3$) S form in **3.** This observation is in opposition to the data obtained for T$_{\mathrm{PO}}$(5′*S*)cdA, in which sugar moiety of thymidine adopts ($^3T_4$) N conformation[13] (Table 1). It should be mentioned that this change originates from the fact that the calculations were carried out for the gas phase.

Table 1
Value of torsion angles and pseudorotation parameters in the sugar moiety (DFT method B3LYP/6-31G**)

Angle		Torsion angle value (°)				
		cdA		(5′*R*) cdA$^{\mathrm{NBz}}_{\mathrm{TBDMSi}}$	T$_{\mathrm{PO}}$(5′*R*)cdA	
		(5′*S*)[a]	(5′*R*)		T	cdA
$O^{4'}$–$C^{1'}$–N^1–C^2	χ				−123.9	
$C^{4'}$–$O^{4'}$–$C^{1'}$–$C^{2'}$	ϕ_0	48.1	48.9	48.7	−20.7	48.0
$O^{4'}$–$C^{1'}$–$C^{2'}$–$C^{3'}$	ϕ_1	−36.0	−36.5	−36.5	35.4	−31.6
$C^{1'}$–$C^{2'}$–$C^{3'}$–$C^{4'}$	ϕ_2	10.8	11.0	11.0	−35.9	4.8
$C^{2'}$–$C^{3'}$–$C^{4'}$–$O^{4'}$	ϕ_3	16.9	17.1	16.9	25.0	22.9
$C^{3'}$–$C^{4'}$–$O^{4'}$–$C^{1'}$	ϕ_4	−40.7	−41.5	−41.0	−2.8	−44.5
$C^{3'}$–$C^{4'}$–$C^{5'}$–C^8	τ	68.3	67.4	67.4		70.5
$O^{4'}$–$C^{1'}$–N^9–C^4	χ	−149.6	−153.3	−153.0		−150
Pseudorotation parameters						
Phase	P	283.2	283.2	283.3	165.6	275.6
Amplitude	$\phi_{\max}$	47.4	47.8	47.8	37.0	49.2
Puckering		$_0T^1$	$_0T^1$	$_0T^1$	$^2T_3$	$_0T^1$

[a] Data taken directly from the literature.[13]

2.3. cdA, dA$^{\mathrm{NBz}}_{\mathrm{TBDMSi}}$ and T$_{\mathrm{PO}}$cdA structure determination by NMR spectroscopy

2.3.1. Conformational features of 2-deoxyribose moiety

In the following step, the quantum calculations have been completed using the data obtained from NMR investigations of the molecular structures of **1**, **2** and **3**. In particular, for the determination of the influence of the (5′*R*)cdA on the global geometry and flexibility of the modified oligonucleotide, ^{1}H NMR investigations have been performed. NMR signals collected at 29 °C were used for the determination of the chemical shifts via straightforward 2D COSY[14] NMR experiments. The set of data, which was obtained, constituted as the starting point for further investigations (Table 2). Following a previous study,[13] it was expected that changes should be observed in the sugar moiety of the nucleoside adjacent to the (5′*R*)cdA. The conformation of the furanose ring of thymidine should not correspond to the (*S*)-form. Moreover, the introduction of the substituents at the O3′ and N6 positions of the cdA moiety should facilitate the formation of other more or less probable con-

Table 2
Chemical shifts [ppm] of sugar and base protons from 300 MHz ^{1}H NMR spectra at 29 °C in D_2O

Proton	$(5'R)$cdA[a]	$(5'R)\text{cdA}^{\text{NBz}}_{\text{TBDMSi}}$	$T_{PO}(5'R)$cdA	
			T_{PO}	cdA
1′	6.54	6.62	6.24	6.64
2′	2.56	2.53	2.31	2.60
2″	2.21	2.31	2.60	2.25
3′	4.45	4.34	4.79[b]	4.52
4′	4.75	4.62	4.16	4.98
5′	4.89	4.97	3.76	5.37
5″			3.71	
2	8.12	8.76		8.23
5			1.85	
6			7.61	

[a] Proton chemical shifts of $(5'R)\text{cdA}^{\text{NBz}}_{\text{TBDMSi}}$ obtained in $CDCl_3$.
[b] Obscured by signal from HDO.

formations. In fact, no significant changes in the vicinal proton coupling constants were observed for the cdA units of **1**, **2** and **3,** the largest variation being 0.9 Hz for H3′–H2′ (Table 3), which corresponds to a change in the dihedral angle by ca. 3.7°. Moreover, the chemical shifts of sugar moiety protons of cdA exhibit almost the same value independent of the NMR solvent. The largest differences of the chemical shifts, for protons in cdA, were observed for N2 and C5′ protons and amount to 0.64 and 0.48 ppm, respectively. This difference is the result of changes in the electron-withdrawing effect of the substituents in the nearest environment. Emphasis should be placed on the fact that 5′ adjacent to the nucleoside adopts a $^{1}T_{2}$ conformation, which is characteristic of B-DNA. This is contrary to the data (DFT study) previously obtained for the (5′*S*)-diastereomer of cdA, and was additionally confirmed by the presented theoretical study.

Table 3
Vicinal coupling constants $^{3}J_{H-H}$ (Hz) obtained at 29 °C for the sugar moieties of investigated compounds

	$(5'R)$cdA	$(5'\,R)\text{cdA}^{\text{NBz}}_{\text{TBDMSi}}$	$T_{PO}(5'R)$cdA	
			T_{PO}	cdA
1′–2′	<0.2	<0.2	6.3	<0.2
1′–2″	4.9	4.6	7.0	4.7
2′–2″	−13.9	−13.6	−15.24	−13.7
3′–2′	7.5	7.0	6.7	7.9
3′–2″	4.5	4.6	3.2	4.4
3′–4′	<0.2	<0.2	3.4	<0.2
4′–5′	<0.2	<0.2	3.6	<0.2
4′–5″			4.5	
5′–5″			−12.6	

2.3.2. The orientation of the hydroxyl group with respect to the γ-bond

The spatial orientation around the C4′–C5′ bond should have the most pronounced influence on the geometry of the 5′ internucleotide phosphodiester linkage. The frequency of the distribution of three possible staggered conformers, *g+* (*gauche +*), *t* (*trans*) and *g−* (*gauche −*), is not equivalent. Their populations depend on the sugar puckering, which is strongly connected to the substituents presented in different positions of the nucleoside. This situation does not concern 5′,8-cyclo-2′-deoxyadenosine due to the presence of a new covalent bond between C5′ and C8, which locks the rotation of 5′-OH around the C4′–C5′ bond, therefore determining a *gauche*—conformer for (5′*S*)cdA and a *trans*-conformer for (5′*R*)cdA. For a natural nucleoside, the conformer populations have been estimated from the coupling constants between H4′ and H5′, H5″ using the method described by Westhof et al.[15] It was found that in **3** the population of *g+*, *t* and *g*– conformers was 55%, 28% and 17%, respectively. This means that in the investigated structures, the S-type of the sugar pucker is most abundant for the normal nucleosides on the 5′ end. Moreover, these results are in agreement with the estimation of the conformers. This was achieved regarding the values of $^{3}J_{H-H}$ measured by ^{1}H NMR and using the following equation:

$X_S = 100(J_{1'2'}/9.3)$; $K_{eq} = S/N = J_{1'2'}/J_{3'4'}$ (for (5′*R*)cdA $X_S = 67.7$ and $K_{eq} = 1.9$).

Finally, ^{1}H–^{31}P coupling constants were assigned with the aim of determining the dihedral angles in C4′–C3′–O3′–P and P–O5′–C5′–C4′ using the suitable Karplus equation[16] parameterized by Mooren.[17,18] Unfortunately, due to the overlap of the signal from HDO and 3′H from the thymidine unit, only the constant coupling $^{3}J_{H5'-P}$ for the P—O5′–C5′–C4′ dihedral angle was measured, and this corresponded to 160°.

2.3.3. Determination of the sugar moiety conformation by 2D NOESY experiments

In order to elucidate these results further and to verify the proposed working hypothesis, attempts were made to determine the distances between the sugar protons by 2D NOESY[19] experiments, at 29 °C (Table 4). From these data and with the help of the molecular mechanistic calculations,[20] a three-dimensional structure of compound **3** can be obtained by providing the previously determined distances.

Table 4
Selected distances of sugar protons calculated by DFT B3LYP 6-31G** level and from 2D NOESY NMR experiment

System	Inter-molecular distances (Å) between inter-ring protons							
	$(5'R)\ \text{cdA}^{\text{NBz}}_{\text{TBDMSi}}$		$(5'R)$cdA		$T_{PO}(5'R)$cdA			
					T		cdA	
	DFT	NMR	DFT	NMR	DFT	NMR	DFT	NMR
1′–2′	2.8	2.7	2.8	2.9	3.1	3.0	2.8	2.7
1′–2″	2.5	2.4	2.5	2.5	2.4	2.4	2.5	2.4
2′–3′	2.4	2.3	2.4	2.5	2.4	2.3	2.4	2.3
2″–3′	3.0	2.9	3.0	2.8	2.7	2.8	3.0	3.0
3′–4′	2.9	2.7	2.8	2.9	2.8	3.0	2.8	2.8
3′–5′	2.4	2.4	2.6	2.4			2.5	2.5
4′–5′	2.6	2.5	2.6	2.7	2.4	2.4	2.6	2.6

The conformation of the five-membered ring is described using the pseudorotation concept developed by Kilpatrick. Thus, the relationship between the five torsion angles (Fig. 1) determined the phase (P) and the amplitude of the sugar unit[21] (Table 5). It has been shown that the sugar in (5′*R*)cdA adopts an unusual W-west conformation, $_{0}T^{1}$. Moreover, it can be inferred when considering the $^{3}J_{H-H}$ data obtained for the investigated derivatives that the conformation of the rigid (5′*R*)cdA unit is not affected by substituents in different positions. Contrary to (5′*S*)cdA in the NMR spectra of (5′*R*)cdA and investigated derivatives, the characteristic H5′;H3′ interaction was present (Table 4). In addition, the results obtained suggest that the 5′-end sugar of the nucleosides attached to cdA predominantly adopts an (*S*)-conformation. Moreover, this observation has been confirmed by its existence in the 2D NOESY spectra of a cross-peak corresponding to 2.5 Å distance between H6 and H2′ of the thymidine unit with the absence of signals from H6–H2″ and H6–H1′ interactions.

Based on the data derived from the aforementioned measurements and calculations, it was possible to build three-dimensional models of **1, 2** and **3.** Figure 3B presents the deduced structure of the most significant compound **3,** $T_{PO}(5'R)$cdA.

From data currently available in literature,[22] it is known that $T_{PO}(5'S)$cdA is not fully depredated to free nucleosides by enzymes. These results suggest that the (*S*)-diastereoisomer blocks the

Table 5
Value of inter-sugar dihedral angles, sugar conformation phase *P* and amplitude ϕ_{max} of sugar calculated from 2D NOESY NMR experiments

Angle		Torsion angle value (°)				
		cdA		$(5'R)$ cdA$^{NBz}_{TBDMSi}$	$T_{PO}(5'R)$cdA	
		$(5'S)$[a]	$(5'R)$		T	cdA
$O^{4'}$–$C^{1'}$–N^9–C^2	χ[b]				60.4	
$C^{4'}$–$O^{4'}$––$C^{1'}$–$C^{2'}$	ϕ_0	45.2	48.3	43.6	−10.0	45.9
$O^{4'}$–$C^{1'}$–$C^{2'}$–$C^{3'}$	ϕ_1	−27.3	−37.2	−26.3	18.2	−30.5
$C^{1'}$–$C^{2'}$–$C^{3'}$–$C^{4'}$	ϕ_2	1.3	4.2	1.6	−18.2	4.0
$C^{2'}$–$C^{3'}$–$C^{4'}$–$O^{4'}$	ϕ_3	25.1	23.9	23.3	13.1	23.0
$C^{3'}$–$C^{4'}$–$O^{4'}$–$C^{1'}$	ϕ_4	−44.8	−44.9	−42.0	−2.1	−42.6
$C^{3'}$–$C^{4'}$–$C^{5'}$–C^8	τ[b]		71.2	74.5		67.3
$O^{4'}$–$C^{1'}$–N^9–C^4	χ[b]		−148.1	−149.5		−159
Pseudorotation parameters						
Phase (P)		272	275	272	166	275
Amplitude (ϕ_{max})		37	48	46	19	46
Puckering		${}_0T^1$	${}_0T^1$	${}_0T^1$	${}^2T_3$	${}_0T^1$

[a] Data taken directly from the literature.[13]

[b] Value obtained after molecular mechanics calculations with distances inferred from 2D NOESY experiments.

hydrolytic activity of *endo*- or *egzo*-nucleases. Moreover, from a study reported by Cadet et al., it is known that (5′*S*)cdA completely blocks the polymerization process of DNA chain.[8] On the other hand, polymerase Polη could bypass (5′*R*)cdA, which is present in the matrix chain of DNA.[8] As mentioned in the introduction, 5′8-cyclo-2′-deoxynucleosides are substrates for the nucleotide repair system, but the (*R*)-diastereomer is being more efficiently removed from genome than the (*S*)-diastereomer.[23] These data suggest that the presence of different isomeric forms of cdA in the genome leads to various results. From a chemical-physical point of view, the influence of the stereogenic centre at C5′ of 5′,8-cyclo-2′-deoxyadenosine can be well demonstrated by a simple RP-HPLC analysis. The (5′*R*)cdA and T_{PO}(5′*R*)cdA exhibit a shorter retention time than the relative derivatives of the opposite diastereoisomer; surprisingly, T_{PO}(5′*R*)cdA is eluted faster than natural 2′-deoxyadenosine (Fig. 3A).

This observation can be used to explain the different biological consequences described above. To explain these phenomena, molecular mechanics calculations of the investigated dinucleotides were performed at a periodic box of water.[24] As a starting point for this study, the d[T_{PO}A] was extracted from ds-DNA.[25] The modified dinucleosides T_{PO}(5′*S*)cdA and T_{PO}(5′*R*)cdA were obtained by a suitable rearrangement of d[T_{PO}A]. As presented in Figure 4, T_{PO}(5′*R*)c-dA has shown a related structure to d[T_{PO}A], and due to this feature it probably has been better recognized by enzymes. Moreover, the diagnostic distance between H2 of adenine and H3 of thymine from d[T_{PO}A] was 3.06 Å; the same distances for T_{PO}cdA containing the (5′*R*)- and (5′*S*)-diastereomer of cdA were 5.58 Å and 6.45 Å,

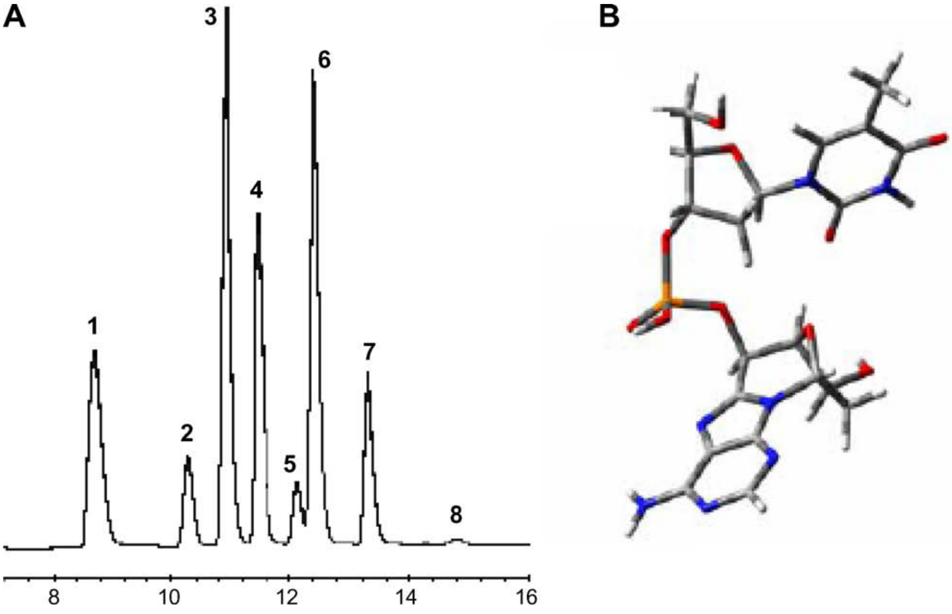

Figure 3. (A) Reverse-phase HPLC analysis of the mixture of natural 2′-deoxynucleosides (1—dC, 3—dG, 4—T, 7—dA), 5′,8-cyclo-2-deoxyadenosine (2—5′*R*, 5—5′*S*), dinucleotides (6—T_{PO}(5′*R*)cdA, 8—T_{PO}(5′*S*)cdA); (B) three-dimensional structure of T_{PO}(5′*R*)cdA inferred from NMR data.

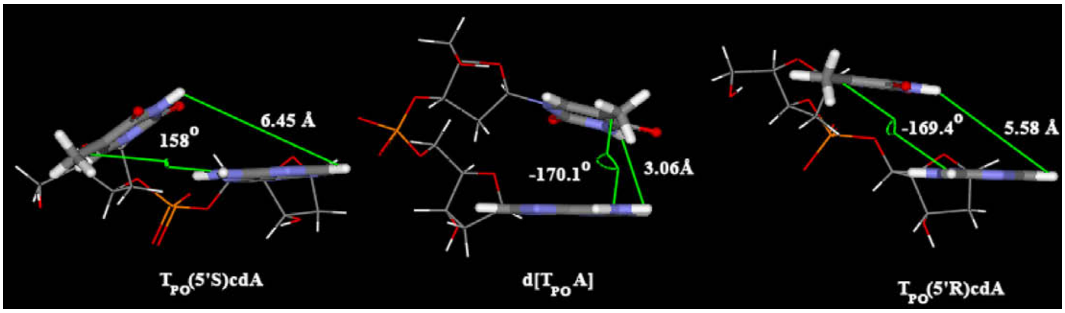

Figure 4. Graphical visualization of the difference in 3D structure between T_{PO}(5′*S*)cdA, d[T_{PO}A] and T_{PO}(5′*R*)cdA obtained by molecular mechanics calculation in a periodic box of water.

respectively. Additionally, the dihedral angel determined by N9–C8 from adenine and N1–C2 from thymine, which described the arrangement between neighbouring bases, was −170.1° for d[T_{PO}A], and −169.4° and 158.2°, respectively, for T_{PO}(5′*R*)cdA and T_{PO}(5′*S*)cdA.

3. Conclusion

In conclusion, (5′*R*)cdA as a model of the tandem base modification occurring in DNA as the result of an ionization radiation or an oxidative stress has been synthesized and studied by NMR and DFT. It has been demonstrated that the covalent bond between C5′ and C8 in the nucleoside induces an unusual West conformation ($_0T^1$) of the furanose ring. Moreover, the postulated geometry is independent of the substituents on the furanose ring and in the adenine moiety. It should be pointed out that despite the changes in the configuration on C5′ atom (*S*→*R*), the sugar conformation remains the same—$_0T^1$. The excellent agreement between the available crystallographic, DFT and NMR data should also be noted. As a result, they converge to essentially the same puckering, amplitude of sugar moiety and distances between protons in investigated molecules.

The results strongly indicate that the sugar's 5-membered ring adopts the same conformations for 2′-deoxynucleosides with a rigid geometry. Moreover, from previous[13] and present data, it was found that the structure of the (*S*)- and (*R*)-diastereomer of 5′,8-cyclo-2′-deoxyadenosine is probably both temperature and derivatization independent. In the ^{1}H NMR experiments at 29 °C, no significant changes in the values of $^3J_{H-H}$ have been observed for (5′*R*)cdA, (5′*R*)cdA$^{NBz}_{TBDMSi}$ and dT_{PO}(5′*R*)cdA, as in the case of previously studied derivatives of ((5′*S*)cdA).[13] Finally, by combining 2D NOESY experiments with simple molecular mechanics calculations and using fixed inter-proton distances, it has been demonstrated that the 5′-end sugar residue of nucleosides **3** predominately adopts an (*S*)-conformation, namely $^2T_3$. In the same way, the conformation of the furanose five-membered ring of (5′*R*)cdA derivatives adopts a $_0T^1$ conformation. It can therefore be postulated that the rigid and fixed structure of cdA can strongly influence the global geometry of oligonucleosides. Moreover, by comparison of the obtained three-dimensional structure of d[T_{PO}A] with T_{PO}(5′*R*)cdA and T_{PO}(5′*S*)cdA by molecular mechanics study, it has been found that (5′*R*)-derivatives adopt a structure more related to natural dinucleotide T_{PO}dA than the opposite (5′*S*)-diastereomer.

4. Experimental

4.1. Synthesis of cdA, cdA$^{NBz}_{TBDMSi}$ and T_{PO}cdA

The (5′*R*)-5′,8-cyclo-2′-deoxyadenosine **1,** cdA$^{NBz}_{TBDMSi}$ **2** and derivatives for short oligonucleotides synthesis were obtained by a method described by Cadet.[8] Dinucleotides T_{PO}cdA **3** were synthesized according to the solid-phase synthesis approach on a 1 μmol scale using the classical phosphoramidite strategy[9] with the slight modification reported by Brooks et al.[10] The synthesized products were purified in one-step RP-HPLC in the DMT^{OFF} mode. For this purpose, a Supelco column, Discover® RP-C18 (25 cm × 4.6 mm, 5 μm), was used. The elution was by achieved using 0.1 M ammonium acetate (AA) as the buffer A with a gradient for compound **1** from 0% to 10% of acetonitrile in 25 min, and for compounds **3** from 0% to 14% of acetonitrile in 25 min; detection λ = 260 nm; the chromatogram presented in Figure 3A was achieved using buffer A with a gradient from 0% to 100% of buffer B (40% acetonitrile in buffer A) in 30 min, retention times, given in minutes, observed in the elution profile: 8.7(1-dC), 10.27 (2-(5′*R*)cdA), 10.92 (3-dG), 11.5 (4-T), 12.1 (5-(5′*S*)cdA), 12.4 (6-T_{PO}(5′*R*)cdA), 13.31 (7-dA), 14.8 (T_{PO}(5′*S*)cdA).

(5′*R*)cdA$^{NBz}_{TBDMSi}$ **1** yield of inversion of configuration step ((5′*S*)cdA$^{NBz}_{TBDMSi}$→(5′*R*)cdA$^{NBz}_{TBDMSi}$) described by the J. Cadet group[26] 20%; (5′*R*)cdA **2** RP-HPLC R_t = 15,0 min; UV (H_2O) λ_{max} = 267 nm; T_{PO}(5′*R*)cdA **3**; yield 80% (under HPLC integration), RP-HPLC R_t = 15.5 min; UV (H_2O) λ_{max} = 267 nm; *m*/*z* (MALDI ToF) 552.1 ($[M-H]^-$, requires 552.42); ^{31}P NMR (D_2O) δ: −1.2 ppm.

4.2. Computation methodology

4.2.1. Quantum mechanics study

The molecular structure of the (5′*R*)cdA **1**, (5′*R*) cdA$^{NBz}_{TBDMSi}$ **2** and T_{PO}cdA **3** was calculated using a DFT (Density Functional Theory) approach with B3LYP (Becke's three-parameter exchange functional and the gradient-corrected functional of Lee, Yang and Parr). For **1**, **2** and **3,** the 6-31G** base was used. The calculation of all structures was achieved with GAUSSIAN 03 Revision D.01.[27]

4.2.2. Molecular mechanics study

The structures of **1**, **2** and **3** were calculated using HyperChem 8.0 software, evaluation version, (HyperCube, Inc.), using MM+ molecular force files, RMS gradient 0.001 Kcal/mol, the Polak-Ribiere Conjugate Gradient Algorithm; also the periodic box 20/20/20 Å (*w*/*h*/*d*) was used. The minimum distance between the solvent and solute atom was 2.3 Å.

4.3. NMR parameters

All NMR spectra were recorded on a Varian 'Mercury 300' (300 MHz) spectrometer. ^{1}H spectra were recorded at 29 °C and collected in 65.3 K data points including 500 transients; the spectra width was 3108 Hz at an operation frequency of 300.1 MHz.

^{31}P spectra were acquired at 29 °C in 20.5 K, over 128 transients with a spectral width of 10000 Hz and an operating frequency of 121.5 MHz.

^{1}H spectra were referenced to the residual HOD of D_2O fixed at 4.80 ppm.

2D COSY spectra and 2D NOESY spectra were obtained by a standard puls-programme implemented in the standard VARIAN software.

The distances between suitable protons were obtained from 2D NOESY experiments. In NOESY spectra, the intensity of cross-peaks is related to the distances between spins via the relaxation matrix.[14] For the distances assignment, the following equation was used $r_{ij} = r_{ref}\ (I_{ref}/I_{ij})^{1/6}$, where r_{ref} is the reference distance. This is usually done with the help of a reference NOE corresponding to a known distance. For compounds **1**, **2** and **3,** as a reference (r_{ref}), distance between H-2′ and H-2″ from CH_2 group was used (r_{ref} = 1.78 Å). For compound **3,** as an additional reference, the distance between the H-6 and CH_3 proton of thymine was used (r_{ref} = 2.70 Å).[28] As an $I_{ref,}$ the integration of the cross-peak corresponding to the known distance (r_{ij}) was assigned as **1**.

All spectra were processed on a personal computer after accumulation, using MESTRENOVA 5.2.3 (Mestreclab Research) software.

Acknowledgement

I would like to thank the Medical University of Lodz (502-13-704) for support.

References

1. (a) Burrows, C. J.; Muller, G. J. *Chem. Rev.* **1998**, *98*, 1109–1152; (b) Knapp, W.; Pogozelski, B.; Tullius, D. T. *Chem. Rev.* **1998**, *98*, 1089–1108.
2. Cadet, J.; Douki, T.; Gasparutto, D.; Ravanat, J.-L. *Mutat. Res.* **2003**, *531*, 5–23.

3. Sancar, A.; Lindsey-Boltz, L.; Unsal-Kacmaz, K.; Linn, S. *Annu. Rev. Biochem.* **2004**, *73*, 39–85.
4. Scancar, A. *Chem. Rev.* **2003**, *103*, 2203–2238.
5. Dizdaroglu, M.; Jurga, P.; Rodrigez, H. *Free Radic. Biol. Med.* **2001**, *30*, 774–784.
6. Brooks, P. J. *DNA Repair* **2008**, *7*, 1168–11799.
7. Kuraoka, I.; Robins, P.; Masutani, C. H.; Hanaoka, F.; Gasparutto, D.; Cadet, J.; Wood, R. D.; Lindahl, T. *J. Biol. Chem.* **2001**, *276*, 49283–49288.
8. Romieu, A.; Gasparutto, D.; Molko, D.; Cadet, J. *J. Org. Chem.* **1998**, *63*, 5245–5249.
9. Romieu, A.; Gasparutto, D.; Cadet, J. *Chem. Res. Toxicol.* **1999**, *12*, 412–421.
10. Brooks, P. J.; Wise, D. S.; Berry, D. A.; Kosmoski, V. J.; Smerdon, M. J.; Somer, R. L.; Mackie, H.; Spoonde, A. Y.; Ackerman, E. J.; Coleman, K.; Taronc, R. E.; Robbins, J. H. *J. Biol. Chem.* **2002**, *275*, 22355–22362.
11. Birnbaum, G. I.; Cygler, M.; Dudycz, L.; Stolarski, R.; Shugar, D. *Biochemistry* **1981**, *20*, 3294–3301.
12. Shishkin, O. V.; Pelmenschikov, A.; Hovorun, M. D.; Leszczynski, J. *J. Mol. Struct.* **2000**, *526*, 326–341.
13. Karwowski, B. T.; Gaillard, J.; Grand, A.; Cadet, J. *Org. Biomol. Chem.* **2008**. DOI: 101039/b807046f.
14. Wijmenga, S. S.; van Buuren, B. N. M. *Prog. Nucl. Magn. Reson. Spectrosc.* **1998**, *32*, 287–387.
15. Westhof, E.; Roder, O.; Croneiss, L. I.; Ludeman, H.-D. *Z. Naturforsch. Teil C.* **1975**, *30*, 131–140.
16. Davis, D. B.; MacCoss, M.; Danyluk, S. S. *J. Chem. Soc., Chem. Commun.* **1984**, *8*, 536–538.
17. Mooren, M. M.; Wijmenga, S. S.; van der Marel, G. A.; van Boom, J. H.; Hilbers, C. W. *Nucleic Acids Res.* **1994**, *22*, 2658–2666.
18. Wijmenga, S. S.; Mooren, M. M.; Hilbers, C. W. In *NMR of Macromolecules, A Practical Approach ed.*; Roberts, G. C. K., Ed.; Oxford University Press: New York, 1993.
19. Gochin, M.; James, T. *Biochemistry* **1990**, *29*, 11172–11180.
20. Wang, J.; Kollman, A. P. *J. Comput. Chem.* **2001**, *22*, 1219–1228.
21. Houseknecht, B. J.; Altona, C.; Hadad, Ch. M.; Lowary, T. L. *J. Org. Chem.* **2002**, *67*, 4647–4651.
22. Jaruga, P.; Theruvathu, J.; Dizdaroglu, M.; Brooks, P. J. *Nucleic Acids Res.* **2004**, *32*, e87. doi:10.1093/nar/gnh087.
23. Jaruga, P.; Dizdaroglu, M. *DNA Repair* **2008**. doi: 10.1016/j.dnarep.2008. 06.005.
24. Zacharias, M. In *Computational Study of DNA and RNA*; Sponer, J., Lankas, F., Eds.; Springer: Berlin, 2006; pp 95–120.
25. Goodsell, D. S.; Kaczor-Grzeskowiak, M.; Dickerson, R. E. *J. Mol. Biol.* **1994**, *240*, 79–96.
26. Romieu, A.; Gasparutto, D.; Cadet, J. *Chem. Res. Toxicol.* **1999**, *12*, 412–421.
27. Frisch, M. J.; Trucks, G. W.; Schlegel, H. B.; Scuseria, G. E.; Robb, M. A.; Cheeseman, J. R.; Montgomery, J. A.; Vreven, T. Jr.; Kudin, K. N.; Burant, J. C.; Millam, J. M.; Iyengar, S. S.; Tomasi, J.; Barone, V.; Mennucci, B.; Cossi, M.; Scalmani, G.; Rega, N.; Petersson, G. A.; Nakatsuji, H.; Hada, M.; Ehara, M.; Toyota, K.; Fukuda, R.; Hasegawa, J.; Ishida, M.; Nakajima, T.; Honda, Y.; Kitao, O.; Nakai, H.; Klene, M.; Li, X.; Knox, J. E.; Hratchian, H. P.; Cross, J. B.; Bakken, V.; Adamo, C.; Jaramillo, J.; Gomperts, R.; Stratmann, R. E.; Yazyev, O.; Austin, A. J.; Cammi, R.; Pomelli, C.; Ochterski, J. W.; Ayala, P. Y.; Morokuma, K.;. Voth, G. A; Salvador, P.; Dannenberg, J. J.; Zakrzewski, V. G.; Dapprich, S.; Daniels, A. D.; Strain, M. C.; Farkas, O.; Malick, D. K.; Rabuck, A. D.; Raghavachari, K.; Foresman, J. B.; Ortiz, J. V.; Cui, Q.; Baboul, A. G.; Clifford, S.; Cioslowski, J.; Stefanov, B. B.; Liu, G.; Liashenko, A.; Piskorz, P.; Komaromi, I.; Martin, R. L.; Fox, D. J.; Keith, T.; Al-Laham, M. A.; Peng, C. Y.; Nanayakkara, A.; Challacombe, M.; Gill,, P. M. W.; Johnson, B.; Chen, W.; Wong, M. W.; Gonzalez, C.; Pople, J. A.; Gaussian, Inc., Wallingford CT, 2004.
28. Gronenborn, A. M.; Clore, G. M. *Prog. NMR Spectrosc.* **1985**, *17*, 1–32.